

E13-2017-95

M. Turek¹, D. Maczka², A. Drozdziel¹,
K. Pyszniak¹, Yu. V. Yushkevich,
Yu. A. Vaganov, P. Wegierek³

INFLUENCE OF THE PENNING IONIZATION
ON ION SOURCE EFFICIENCY —
NUMERICAL SIMULATIONS

¹ Institute of Physics, M. Curie-Skłodowska University, Lublin, Poland

² National Center for Nuclear Research, Swierk, Poland

³ Lublin University of Technology, Lublin, Poland

Турек М. и др.

E13-2017-95

Влияние ионизации Пеннинга на эффективность
ионного источника — численные моделирования

Представлена численная модель ионизации в плазменном источнике ионов, которая учитывает ионизацию электронным ударом и эффект Пеннинга. Исследуется влияние эффекта Пеннинга на эффективность ионизации. Показано, что газ-носитель может в несколько раз увеличить эффективность ионизации по сравнению с вариантом чисто электронной ионизации. Изменения выхода с учетом ионизации Пеннинга исследовались как функция концентрации газа-носителя, степени ионизации и концентрации атомов газа-носителя в метастабильном состоянии.

Работа выполнена в Лаборатории ядерных проблем им. В. П. Дзепелова ОИЯИ и в Институте физики Университета им. М. Кюри-Склодовской (Люблин).

Сообщение Объединенного института ядерных исследований. Дубна, 2017

Turek M. et al.

E13-2017-95

Influence of the Penning Ionization on Ion Source Efficiency —
Numerical Simulations

A numerical model of ionization in the plasma ion source, allowing for the electron impact and Penning effect, is presented. The influence of the Penning effect on the ionization efficiency is investigated. It is shown that the carrier gas can improve the ionization efficiency several times compared to the pure electron ionization case. Changes of the yield from the Penning ionization are investigated as a function of the carrier gas concentration, degree of ionization, and concentration of carrier gas atoms in the metastable state.

The investigation has been performed at the Dzheleпов Laboratory of Nuclear Problems, JINR, and the Institute of Physics, UMCS, Lublin.

Communication of the Joint Institute for Nuclear Research. Dubna, 2017

INTRODUCTION

Ion source efficiency is a crucial parameter in mass and nuclear spectrometries as well as in other fields. A variety of ion production mechanisms (including electron impact ionization, surface ionization, photon ionization, etc.) are described and employed in ion sources of different designs [1]. In many cases, one of these processes can usually be considered as the dominant one, i.e., the one that contributes the most to the ionization yield of the ion source, as, e.g., electron impact ionization in arc discharge ion sources or surface ionization in hot cavities. However, there could be additional or concurrent processes that affect the performance of the ion source and could, for example, produce ions that are impossible to be created by the main mechanism or contribute to the ion source yield to a great extent. It was experimentally shown that the electron impact ionization takes place in the thermoemission ion sources [2] resulting in multiply charged ion production, which is impossible in the surface process. The fact that the electron impact ionization could be an important (or even dominant) ion production channel in the hot cavity ion source was demonstrated by numerical simulations for both stable [3] and radioactive nuclides [4, 5]. Similarly, free electron capture is the only ionization mechanism that leads to SF₆ negative ion formation in the hot surface ion source [6]. It is also known that two different H⁻ (or D⁻) ion production processes occur in large intensity negative ion sources developed for the International Thermonuclear Experimental Reactor (ITER) plasma heating purposes [7, 8], namely, the surface and volume ionization channels [9]. The influence of the Penning effect on the efficiency of the plasma ion sources was also intensively studied [10–12]. It was found that using a carrier gas like He or Xe could improve ion source efficiency several times due to the Penning ionization during the collisions of Hg atoms with metastable carrier gas atoms.

The paper describes the studies of the influence of the Penning effect on the ionization in the plasma ion source using computer simulations based on the Monte Carlo method. A brief description of the model allowing for both electron and Penning ionization is given. The dependence of the carrier gas (He) ionization efficiency on the carrier gas concentration is studied and compared with the experimental measurements. Changes of the Hg ionization efficiency of both processes with the degree of plasma ionization and carrier gas atoms in the ground and metastable states are investigated. Relative Hg and He ionization efficiency is also calculated and discussed.

PENNING EFFECT

In many cases, especially during ionization of radioactive nuclides, it is necessary to use an additional carrier gas (besides the sample) to maintain a stable discharge in the ion source chamber. This fact offers the possibility of increasing the ionization efficiency by using not only electron impact ionization of the sample atoms (B),



but also other kinds of collisions, including those of sample atoms with the metastable atoms (A^m) of the carrier gas:



The above-mentioned process is called the Penning ionization, and it takes place when the ionization energy of the sample atom is smaller than that of the metastable state of the carrier gas atoms [13]. It should be mentioned that in the considered case the Penning effect happens when the He metastable levels (2^1S_0 and 2^3S_1) are higher (20.6 and 19.8 eV) than the Hg ionization energy (10.4 eV). Atoms in the metastable state are created by collisions with electrons and radiation transitions from the excited states:



Metastable carrier gas atoms are lost not only in the process (2) but also during $A^m + A$ collisions. Concentration of He atoms in the metastable state will be considered further as one of the control parameters of the simulation.

NUMERICAL MODEL

Simulations were done using the test particle tracking approach similar to that presented in [14–16]. The numerical code follows the trajectories of particles inside the ion source chamber. A schematic drawing of the simulated system is shown in Fig. 1. The ionization chamber with the inner diameter of 9 mm is closed with an anode on one side and an endcap with the extraction opening ($r_{\text{ext}} = 0.5$ mm). The simulation area is covered by a 3D ($150 \times 100 \times 100$ cells) rectangular mesh with $\Delta x = \Delta y = \Delta z = 0.1$ mm. The electrostatic potential is found by solving the Laplace equation using the iterative over-relaxation method, as in [14–18], with the boundary conditions determined by the electrode shapes and voltages. The electric field is calculated by the numerical derivation of the electrostatic potential. Particle trajectories are found by the integration of the

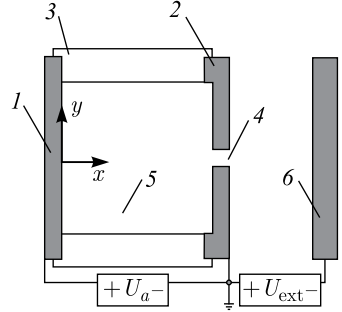


Fig. 1. Schematic view of the simulated system: 1 — anode, 2 — cathode, 3 — insulator, 4 — extraction opening, 5 — ionization chamber, 6 — extraction electrode

classical equations of motion using the fourth-order Runge–Kutta method [19]. Neutral particles are assumed to start their journey inside the circle 3 mm in diameter placed at the distance of 3 mm from the anode. Ionization is implemented using the Monte Carlo formalism similar to that described in [20].

Let us assume that the neutral particle could be ionized in n independent processes. Thus, the total probability of being ionized during a single simulation time step could be estimated as

$$P_{\text{ion}} = 1 - \exp\left(-\sum_{i=1}^n \nu_i \Delta t\right), \quad (4)$$

where ν_i is the frequency of the i th process proportional to its total cross section, density of target particles, and rate. In the considered case $n = 2$, since both the electron impact ionization ($i = 1$) and the Penning ionization ($i = 2$) are taken into account. The electron ionization frequency is estimated as

$$\nu_1 = \sigma_E v n_e, \quad (5a)$$

where σ_E is the electron impact ionization cross section, n_e is electron density, and v is the estimated average relative velocity (since electrons are much faster than neutrals in plasma). As far as the Penning ionization is concerned, there are the reaction rates $\langle \sigma_P v \rangle$ rather than the cross-section values given in the literature [21]. Therefore, it is assumed that

$$\nu_2 = \langle \sigma_P v \rangle n_m, \quad (5b)$$

where n_m is the density of the carrier gas atoms in the metastable state. The electron impact ionization cross sections for Hg are taken from [22]. Ions are neutralized when they hit the electrodes. Ions and neutrals are tracked until they pass the extraction opening. The ionization efficiency is calculated as the ratio of the number of extracted ions to the total number of extracted particles (ions and neutrals) of a given kind (metal or carrier gas ions):

$$\beta_s = N_+ / (N_+ + N_0). \quad (6)$$

SIMULATION RESULTS

Simulations were done for the Hg/He mixtures, as in the experiments [10–12]. The carrier gas density n_{He} varied in the range from $n_{\text{He}0} = 10^{20} \text{ m}^{-3}$ up to 10^{21} m^{-3} . During the experiments Hg vapors were added at a much smaller leak rate ($\sim 0.35 \text{ cm}^3 \cdot \text{Torr} \cdot \text{min}^{-1}$) than the carrier gas ($20\text{--}200 \text{ cm}^3 \cdot \text{Torr} \cdot \text{min}^{-1}$). Hence, the influence of electron density depends mostly on the He atom density.

It was assumed that the electron density was scaled with n_{He} as

$$n_e = x_i n_{\text{He}} u(n_{\text{He}}), \quad (7)$$

where x_i is the initial degree of ionization, considered as a control parameter, and $u(n_{\text{He}}) = (n_{\text{He}0}/n_{\text{He}})^{1/3}$ is chosen to reproduce the experimental $\beta_s(n_{\text{He}})$ dependence [12] (see Fig. 2, *a*). Figure 2, *b* shows the ionization efficiency for the He atoms obtained in simulations for different x_i using $3 \cdot 10^7$ of the test particles. The flat extraction electrode at the potential $V_{\text{ext}} = 1 \text{ kV}$ was placed at the distance of 2.5 mm from the extraction hole. The anode voltage was set to $U_a = 100 \text{ V}$. The simulation time step was $\Delta t = 2 \cdot 10^{-8} \text{ s}$. One can see good qualitative agreement with the experimentally determined trends: the simulation results also follow $n_{\text{He}}^{-1/3}$ curves.

As was already mentioned, Hg atoms could be ionized during both the electron impact and the Penning ionization. The probability of the latter process depends on the density of the carrier gas atoms in the metastable state

$$n_m = x_m n_{\text{He}}, \quad (8)$$

where x_m is another control parameter.

Looking at Eqs. (5), (7) and (8), one may expect that the role of the Penning ionization increases with the carrier gas density. This is confirmed by the results

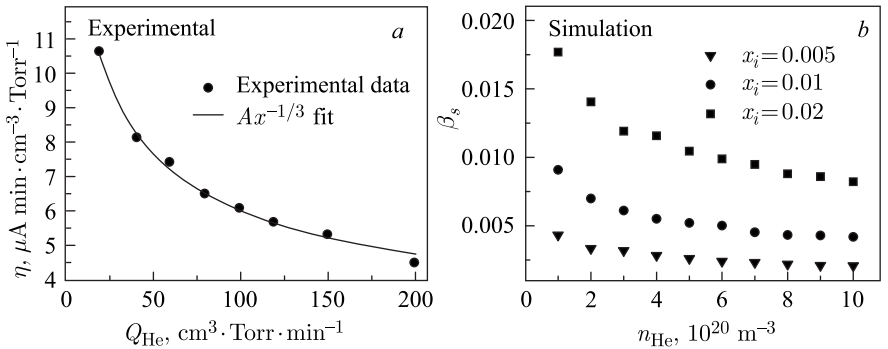


Fig. 2. Efficiency of the carrier gas (He) ionization measured in experiments (*a*) and obtained from simulations (*b*)

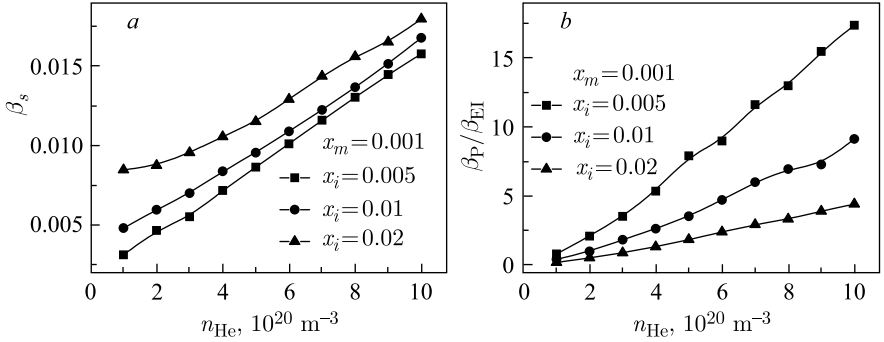


Fig. 3. Hg ionization efficiency as a function of carrier gas concentration calculated for different values of ionization degree (a) and relative efficiency of Penning and electron impact processes (b)

shown in Fig. 3. Calculations were done for $x_m = 0.001$ using $6 \cdot 10^5$ test particles representing Hg atoms. In Fig. 3, a one can see that for larger values of n_{He} the ionization efficiency increases almost linearly, particularly, in the case of a smaller degree of ionization (e.g., $x_i = 0.001$). In such cases, the Penning ionization is dominant, see also the relative contribution of both processes shown in Fig. 3, b. The Penning process contributes several times more strongly than the electron impact ionization even for moderate carrier gas concentrations. The effect of the Penning ionization becomes more important for smaller values of the x_i parameter (degree of ionization). Degree of ionization could be related to such working parameters of the ion source as, e.g., discharge voltage.

On the other hand, for smaller n_{He} and larger x_i the probability of electron impact ionization is comparable to that of the Penning ionization, and the deviation from the linear trend predicted by Eqs. (5) and (8) is significant, see the $\beta_s(n_{\text{He}})$ curve for $x_i = 0.02$. In that case, the $\beta_P/\beta_{\text{EI}}$ ratio is smaller than 1 even for $n_{\text{He}} = 3 \cdot 10^{20} \text{ m}^{-3}$.

The ionization efficiency variation with the density of the carrier gas atoms in the metastable state was also investigated. Figure 4 shows the results obtained for $x_i = 0.01$ and x_m varying from 0.001 to 0.2. The efficiency increases with x_m as could be expected from (8). The increase is almost perfectly linear in the considered range of parameters. The changes in the slope a are presented in Fig. 4, b. The dependence of the slope on the concentration of He atoms in the metastable state is also almost linear, which means that the Penning ionization is the dominant ionization process in the presented case.

Figure 5 shows the relative efficiencies of the sample and the carrier gas ions obtained in both experiment and the simulations. In both cases, one observes a

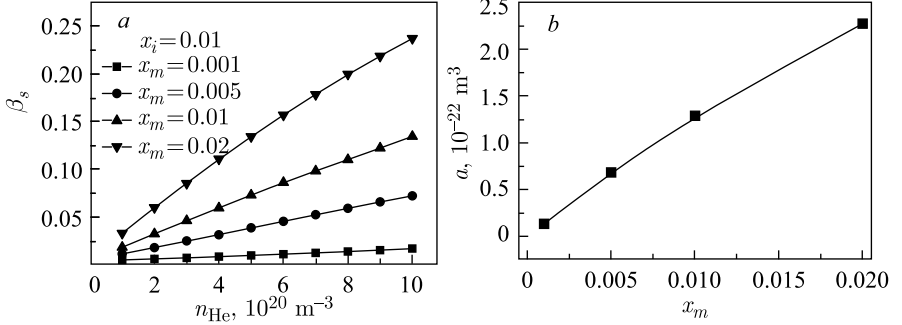


Fig. 4. Hg ionization efficiency as a function of carrier gas concentration calculated for different concentrations of the carrier gas atoms in the metastable state (a) and changes of the $\beta_s(n_{\text{He}})$ slope value with x_m (b)

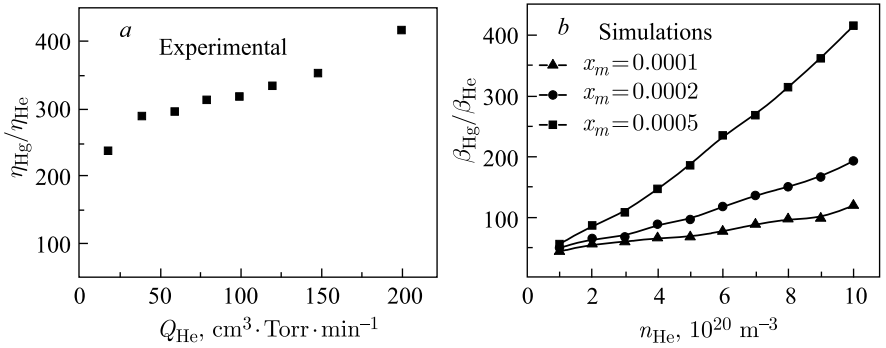


Fig. 5. Relative efficiencies of mercury and helium ion production obtained in experiment (a) and in simulations (b)

nearly linear increase in the relative efficiency with the carrier gas amount. The experimental $\eta_{\text{Hg}}/\eta_{\text{He}}$ values are higher for small Q_{Hg} than that obtained from the simulations. The possible reasons for that are (a) a larger contribution from the electron impact ionization than assumed in the model and (b) more complex dependence of n_m on n_{He} than assumed in Eq. (8).

CONCLUSIONS

A numerical model of ionization in the plasma ion source, taking into account both electron impact and the Penning ionization, is presented. The shape of the ionization efficiency of the carrier gas curves was reproduced by assuming that the electron density scales as $\sim n_{\text{He}}^{2/3}$. It was also shown that according to the

presented numerical model the importance of the Penning effect increases with the carrier gas density. The contribution from the Penning process can be even more than 10 times greater than that from the electron impact ionization (depending on the degree of plasma ionization). The relative ionization efficiency of the sample and carrier gas atoms was also studied. A nearly linear increase with the carrier gas atom concentration was observed, which is in good agreement with the experimental results. Using the carrier gas and employing the Penning effect can be a very simple and effective way of improving the performance of plasma ion sources used for nuclear spectroscopy, ion implantation, isotope separation, etc.

REFERENCES

1. *Brown I.G.* The Physics and Technology of Ion Sources. Berlin: Wiley-VHC, 2004.
2. *Wayne D.M. et al.* // *Int. J. Mass Spectrom.* 2002. V. 216. P. 41.
3. *Turek M., Pyszniak K., Drozdziel A.* // *Vacuum.* 2009. V. 83. P. S260.
4. *Turek M.* // *Acta Phys. Polon. A.* 2014. V. 125. P. 1388.
5. *Turek M.* // *Vacuum.* 2014. V.104. P. 1.
6. *Pelc A.* // *Rapid Commun. Mass Spectrom.* 2012. V. 26. P. 577.
7. *Staebler A. et al.* // *Fusion Eng. Des.* 2009. V. 84. P. 265.
8. *Kraus W. et al.* // *Rev. Sci. Instr.* 2012. V. 83. P. 02B104.
9. *Bacal M., Wada M.* // *Appl. Phys. Rev.* 2015. V. 2. P. 021305.
10. *Maczka D., Gromova I.I., Zuk W.* // *Nucl. Instr. Meth.* 1978. V. 157. P. 483.
11. *Maczka D. et al.* // *Nucl. Instr. Meth.* 1981. V. 186. P. 335.
12. *Maczka D., Meldizon A., Zuk W.* // *J. Phys. D: Appl. Phys.* 1980. V. 13. P. L185-8.
13. *Hasted J.B.* Physics of Atomic Collisions. London: Butterworths, 1964.
14. *Turek M. et al.* // *AIP Conf. Proc.* 2006. V. 812. P. 153.
15. *Pyszniak A. et al.* // *Instr. Exp. Tech.* 2007. V. 50. P. 552.
16. *Turek M. et al.* // *Instr. Exp. Tech.* 2009. V. 52. P. 90.
17. *Turek M., Sielanko J.* // *Vacuum.* 2009. V. 83. P. S256.
18. *Turek M. et al.* // *Nucl. Instr. Meth. B.* 2011. V. 269. P. 700.
19. *Press W.H. et al.* Numerical Recipes in Fortran 77. Cambridge: Cambridge Press Syndicate, 1997.
20. *Vahedi V., Surendra M.* // *Comput. Phys. Commun.* 1995. V. 87. P. 179.
21. *Temelkov K.A., Vuchkov N.K., Sabotinov N.V.* // *J. Phys. Conf. Ser.* 2006. V. 44. P. 116.
22. *Talukder M.R. et al.* // *Eur. Phys. J. D.* 2008. V. 46. P. 281.

Received on December 19, 2017.

Редактор *Е. И. Крупко*

Подписано в печать 08.02.2018.

Формат 60 × 90/16. Бумага офсетная. Печать офсетная.

Усл. печ. л. 0,62. Уч.-изд. л. 0,84. Тираж 215 экз. Заказ № 59333.

Издательский отдел Объединенного института ядерных исследований

141980, г. Дубна, Московская обл., ул. Жолио-Кюри, 6.

E-mail: publish@jinr.ru

www.jinr.ru/publish/